First-principles calculation of correlated electron materials based on Gutzwiller wave function beyond Gutzwiller approximation

First-principles calculation of correlated electron materials based on Gutzwiller wave function beyond Gutzwiller approximation

Zhuo Ye,[1,] Yong-Xin Yao,[1,*] Xin Zhao,[1] Cai-Zhuang Wang,[1] Kai-Ming Ho[1,2]*

[1] Ames Laboratory – US DOE and Department of Physics and Astronomy, Iowa State University, Ames, Iowa 50011, United States

[2] Hefei National Laboratory for Physical Sciences at Microscale, International Center for Quantum Design of Functional Materials (ICQD) and Synergetic Innovation Center of Quantum Information and Quantum Physics, University of Science and Technology of China, Hefei, Anhui 230026, China

Keywords: correlated electron systems, Gutzwiller wave function, potential energy curve

* E-mail: zye@iastate.edu (Z.Y.) ykent@iastate.edu (Y.X.Y.)

ABSTRACT

We propose an approach that is under the framework of Gutzwiller wave function but goes beyond the commonly adopted Gutzwiller approximation to improve the accuracy and flexibility in treating the correlation effects. Detailed formalism is described for a dimer which is straightforwardly generalized later to more complicated periodic bulk systems. The accuracy of the approach is demonstrated by evaluating the potential energy curves of spin-singlet N_2 dimer, spin-triplet O_2 dimer, and one-dimensional hydrogen chain. The computational workload of the approach can be easily handled by efficient parallel computing.

1. INTRODUCTION

Ab initio calculation of correlated electron systems is one of the most fundamental challenges in physics, chemistry and materials science. Understanding and controlling the properties of matter that emerge from their complex correlations of atomic or electronic constituents requires accurate and efficient methods to calculate the energies and properties of strongly-correlated electron materials. While density functional theory (DFT) [1,2] and related computational approaches have been very successful in predicting the structures and properties of many materials, they hardly yield satisfying results for strongly-correlated electron materials. Over the past fifty years, many theories and methods for treating correlated electrons beyond DFT have been proposed and developed, each having different strengths, weaknesses, and domains of applicability. For example, wave function-based quantum chemistry methods, especially the multi-configurational self-consistent field (MCSCF) approaches [3], such as complete active space SCF (CASSCF) [4], or equivalently full-optimized reaction space (FORS) [5,6], and the restrictive active space SCF (RASSCF) [7,8], can be very accurate, and the efficiency of the methods has recently been improved, e.g., by using the density-matrix renormalization group (DMRG) [9-11], but these approaches are still limited to small systems. Quantum Monte Carlo (QMC) methods [12-14] have also advanced significantly in recent years and showcase studies have been available for realistic correlated-electron materials, but the computational workload of QMC remains very heavy. Conversely, hybrid approaches which merge DFT with many-body techniques, e.g., DFT + Hubbard U (DFT+U) [15,16], DFT + dynamical mean-field theory (DFT+DMFT) [17-19], and DFT + Gutzwiller approximation (DFT+G) [20-24], have been demonstrated to be very effective in describing the properties of real correlated-electron materials. However, the use of adjustable screened Coulomb parameters restricts the predictive

power of these methods. It is highly desirable to develop first-principles theories and computational methods for calculating the total energy and electronic structures of correlated-electron materials without using adjustable parameters while retaining computational efficiency, especially for big systems such as big molecules or bulk materials.

Since the seminal work about correlation effects on transition metal ferromagnetism by Gutzwiller in 1960s [25-27], Gutzwiller wavefunctions (GWF) have been widely used in describing strongly correlated systems [20,24,28-31]. The GWF is constructed by applying a correlation operator on the noninteracting wavefunction such that each on-site valence electronic configuration obtains an appropriate amplitude and phase factor [32].

GWF introduces variational parameters directly in the onsite many-body configuration space, rather than an optimized form for the Jastrow function of inter-electron/ion separations [33-36]. Since a closed form of expectation value with respect to GWF is still not generally available, exact evaluations require the variational quantum Monte Carlo simulations, which can be very time-consuming due to large number of variational parameters. Gutzwiller approximation has been introduced to facilitate calculations, which essentially approximates the kinetic energy by including all the hopping processes without pair-environment dependence [27,37]. The approximation was later shown to be equivalent to slave-boson mean field approach [38,39]. The famous applications of Gutzwiller wavefunction based on Gutzwiller approximation include Brinkman-Rice metal-insulator transition and the description of the almost localized fermi liquid behavior of normal ^{3}He [28,40]. While the early calculations were focused on single-orbital Hubbard model (HM), the approach was successfully generalized to multiple correlated orbital systems [41,42]. On the other hand, exact solutions based on GWF are quite scarce. There has been report on 1D single-orbital HM as a first rigorous assessment of the quality of the

Gutzwiller wavefunction [43,44]. It was also proved that Gutzwiller approximation becomes exact in infinite dimension. At finite dimensions, e.g., 3D, the correction terms in single-orbital models have been worked out [45,46], but most calculations are restricted to effective Hamiltonians with on-site Coulomb interactions only. The performance of GWF-based approach when applied to general ab initio many-body Hamiltonian of real systems remains elusive.

Recently, we developed a method, namely, the correlation matrix renormalization (CMR) method which extends the GWF-based approach to the calculation of ground state energy of real correlated-electron materials [47-49]. The CMR method adopts the Gutzwiller variational wave functions and use the Gutzwiller approximation and Hartree-Fock type factorization to treat the intersite Coulomb interactions, thus greatly enhance the computational efficiency. As illustrated in Ref. [49], while the CMR method can achieve a reasonable accuracy for correlated-electron systems, the use of Gutzwiller approximation may still be the major source of inaccuracy. Therefore, a more accurate method that goes beyond the limitation of Gutzwiller approximation is desirable.

In this paper, we propose an approach for accurate evaluation of the total energy and electronic properties of correlated electron systems using GWF but without resorting to the Gutzwiller approximation. We name this approach as Gutzwiller conjugate gradient minimization (GCGM) approach. In GCGM, the total energy is expressed explicitly as a function of the Gutzwiller variational parameters, and is then minimized with conjugate gradient method using analytical energy gradients. The Gutzwiller wavefunction represents a variational many-body wavefunction of relatively simple form, which can be further extended if desired. As we will show later, the GCGM method is more rigorous and flexible to deal with the GWF in some generalized form.

The computational burden for higher accuracies can be released by an efficient partitioning for parallel computing based on the new methodology.

2. METHODS

In the form of second quantization, the full ab initio nonrelativistic Hamiltonian for an interacting many-electron system can be expressed as,

$$H = \sum_{i\alpha j\beta,\sigma} t_{i\alpha j\beta} c^{\dagger}_{i\alpha\sigma} c_{j\beta\sigma} + \frac{1}{2} \sum_{\substack{i\alpha j\beta \\ k\gamma l\delta,\sigma\sigma'}} u(i\alpha j\beta;k\gamma l\delta) c^{\dagger}_{i\alpha\sigma} c^{\dagger}_{j\beta\sigma'} c_{l\delta\sigma'} c_{k\gamma\sigma} \quad (1)$$

where i, j, k, l are the atomic site indices, $\alpha, \beta, \gamma, \delta$ the orbital indices, and σ, σ' the spin indices. Here, t and u are the one-electron hopping integral and the two-electron Coulomb integral, respectively, which can be expressed as,

$$t_{i\alpha j\beta} = \left\langle \phi_{i\alpha} \left| \hat{T} + \hat{V}_{ion} \right| \phi_{j\beta} \right\rangle, \quad (2)$$

$$u(i\alpha j\beta;k\gamma l\delta) = \iint d\mathbf{r} d\mathbf{r}' \phi^{*}_{i\alpha}(\mathbf{r}) \phi^{*}_{j\beta}(\mathbf{r}') \hat{U}(\mathbf{r} - \mathbf{r}') \phi_{l\delta}(\mathbf{r}') \phi_{k\gamma}(\mathbf{r}) , \quad (3)$$

where $\hat{T}$, $\hat{V}_{ion}$, and $\hat{U}$ are the operators for kinetic energy, ion-electron interaction and Coulomb interaction, respectively. $\phi_{i\alpha}$ is the basis orbital at atomic site i with orbital index α. As shown in Eq. (1), all interactions are included in the Hamiltonian without any adjustable parameters. An exact expression of the total energy consisting of one-particle and two-particle density matrices can be obtained if a full configuration interaction (FCI) wave function is used. In our GCGM approach, the total energy is evaluated with the GWF of the form,

$$\left|\Psi_{GWF}\right\rangle = \prod_i \left(\sum_{\Gamma} g(\Gamma_i) \left|\Gamma_i\right\rangle \left\langle \Gamma_i \right| \right) \left|\Psi_0\right\rangle, \tag{4}$$

which is constructed based on the non-interacting wave function $\left|\Psi_0\right\rangle$, i.e. a single Slater determinant. $g(\Gamma_i)$ is the Gutzwiller variational parameter determining the occupation probability of the on-site configuration $\left|\Gamma_i\right\rangle$, which is defined as a Fock at i^{th} site $\left|\Gamma_i\right\rangle \equiv \prod_{\alpha\sigma\in\Gamma_i} c_{\alpha\sigma}^{\dagger} \left|\varnothing\right\rangle$. Here the creation operator $c_{\alpha\sigma}^{\dagger}$ creates an electron at the orbital-α with spin-σ in the vacuum state $\left|\varnothing\right\rangle$. The total energy without adopting Gutzwiller approximation can be expressed as

$$\begin{aligned} E_{GWF} = & \sum_{i\alpha j\beta,\sigma} t_{i\alpha j\beta} \left\langle c_{i\alpha\sigma}^{\dagger} c_{j\beta\sigma} \right\rangle_{GWF} + \frac{1}{2} \sum_{\substack{i,\alpha\beta\gamma\delta \\ \sigma\sigma'}} u(i\alpha i\beta; i\gamma i\delta) \left\langle c_{i\alpha\sigma}^{\dagger} c_{i\beta\sigma'}^{\dagger} c_{i\delta\sigma'} c_{i\gamma\sigma} \right\rangle_{GWF} \\ & + \frac{1}{2} {\sum_{\substack{i\alpha j\beta \\ k\gamma l\delta,\sigma\sigma'}}}' \left(u(i\alpha j\beta; k\gamma l\delta) - \delta_{\sigma\sigma'} u(i\alpha j\beta; l\delta k\gamma) \right) \left\langle c_{i\alpha\sigma}^{\dagger} c_{k\gamma\sigma} \right\rangle_{GWF} \left\langle c_{j\beta\sigma'}^{\dagger} c_{l\delta\sigma'} \right\rangle_{GWF} \end{aligned} \tag{5}$$

where $\sum'$ indicates that the pure on-site terms are excluded from the summation. The on-site two particle correlation matrix (2PCM) are treated rigorously and the intersite 2PCM are evaluated using Hartree-Fock(HF)-type factorized approximation (Wick's theorem, see Ref. [49,50]),

$$\begin{aligned} & \left\langle c_{i\alpha\sigma}^{\dagger} c_{j\beta\sigma'}^{\dagger} c_{l\delta\sigma'} c_{k\gamma\sigma} \right\rangle_{GWF} \approx \\ & \quad \left\langle c_{i\alpha\sigma}^{\dagger} c_{k\gamma\sigma} \right\rangle_{GWF} \left\langle c_{j\beta\sigma'}^{\dagger} c_{l\delta\sigma'} \right\rangle_{GWF} - \delta_{\sigma\sigma'} \left\langle c_{i\alpha\sigma}^{\dagger} c_{l\delta\sigma} \right\rangle_{GWF} \left\langle c_{j\beta\sigma}^{\dagger} c_{k\gamma\sigma} \right\rangle_{GWF} \end{aligned} \tag{6}$$

The following sum-rule correction [49] is also used as in the CMR method, to reduce the HF-type factorization error by effectively evaluating the intersite Coulomb interactions through more accurate onsite calculations,

$$H_{sr} = \frac{1}{2}\sum_{i\alpha}\lambda_{i\alpha}\left(\hat{n}_{i\alpha\sigma}\left(\sum_{j\beta\sigma'}\hat{n}_{j\beta\sigma'} - N_e\right)\right). \tag{7}$$

Here N_e is the total number of electrons in the system and $\lambda_{i\alpha}$ is determined by the weighted average of the relevant intersite 2-electron Coulomb integrals,[1]

$$\lambda_{i\alpha} = -\frac{\sum_{j\neq i,\beta\sigma'} u(i\alpha j\beta; i\alpha j\beta) R_{ij}^{-6}}{\sum_{j\neq i,\beta\sigma'} R_{ij}^{-6}}, \tag{8}$$

where R_{ij} is the distance from atom i to atom j. When we evaluate the energy, we include the sum-rule part H_{sr} in Eq. (7) in the Hamiltonian H in Eq. (1).

For a clear presentation of the method, we consider a dimer that has only 2 sites. The one-particle density matrix (1PDM) can be expressed as,

$$\left\langle c_{i\alpha\sigma}^{\dagger} c_{i\beta\sigma}\right\rangle_{GWF} = \frac{1}{\left\langle \Psi_{GWF}\middle|\Psi_{GWF}\right\rangle}\sum_{\Gamma_i,\Gamma'_i,\Gamma_j}\left\langle \Gamma_i\middle|c_{i\alpha\sigma}^{\dagger}c_{i\beta\sigma}\middle|\Gamma'_i\right\rangle g(\Gamma_i)g(\Gamma'_i)g(\Gamma_j)^2\,\xi^0_{\Gamma_i,\Gamma_j,\Gamma'_i,\Gamma_j}, \tag{9}$$

$$\left\langle c_{i\alpha\sigma}^{\dagger} c_{j\beta\sigma}\right\rangle_{GWF} = \frac{1}{\left\langle \Psi_{GWF}\middle|\Psi_{GWF}\right\rangle}\sum_{\Gamma_i,\Gamma_j,\Gamma'_i,\Gamma'_j}\left\langle \Gamma_i\middle|c_{i\alpha\sigma}^{\dagger}\middle|\Gamma'_i\right\rangle\left\langle \Gamma_j\middle|c_{j\beta\sigma}\middle|\Gamma'_j\right\rangle\cdot \\ g(\Gamma_i)g(\Gamma_j)g(\Gamma'_i)g(\Gamma'_j)\xi^0_{\Gamma_i,\Gamma_j,\Gamma'_i,\Gamma_j} \quad for\ i\neq j \tag{10}$$

where $\xi^0_{\Gamma_i,\Gamma_j,\Gamma'_i,\Gamma_j}$ is predetermined coefficient from $\left|\Psi_0\right\rangle$,

[1] The specific form of Eq. (8) is not unique. It works as long as the weight decreases sufficiently fast with respect to the inter-atomic separations. In other words, the dominant contribution comes from the nearest neighbors.

$$\xi^0_{\Gamma_i,\Gamma_j,\Gamma'_i,\Gamma_j} = \langle \Psi_0 | \Gamma_i, \Gamma_j \rangle \langle \Gamma'_i, \Gamma'_j | \Psi_0 \rangle \ , \tag{11}$$

and

$$\langle \Psi_{GWF} | \Psi_{GWF} \rangle = \sum_{\Gamma_i,\Gamma_j} \xi^0_{\Gamma_i,\Gamma_j,\Gamma'_i,\Gamma_j} g(\Gamma_i)^2 g(\Gamma_j)^2 \ . \tag{12}$$

The on-site 2PCM can be expressed as,

$$\left\langle c^\dagger_{i\alpha\sigma} c^\dagger_{i\beta\sigma}, c_{i\gamma\sigma}, c_{i\delta\sigma} \right\rangle_{GWF} = \frac{1}{\langle \Psi_{GWF} | \Psi_{GWF} \rangle} \sum_{\Gamma_i,\Gamma'_i,\Gamma_j} \langle \Gamma_i | c^\dagger_{i\alpha\sigma} c^\dagger_{i\beta\sigma}, c_{i\gamma\sigma}, c_{i\delta\sigma} | \Gamma'_i \rangle g(\Gamma_i) g(\Gamma'_i) g(\Gamma_j)^2 \xi^0_{\Gamma_i,\Gamma_j,\Gamma'_i,\Gamma_j} \tag{13}$$

Substituting Eq. (9)-(13) into (5), E_{GWF} can be expressed explicitly as a function of $\{g(\Gamma_i)\}$. E_{GWF} is then minimized with respect to $\{g(\Gamma_i)\}$ with conjugate gradient method after the analytical $\frac{\partial E_{GWF}}{\partial g(\Gamma_i)}$ is evaluated. It is worth noting that the calculation of the gradient of total energy contributes most to the computational burden of GCGM. Fortunately, the calculation of the gradient is readily partitioned with regard to the configuration Γ_i, as the evaluation of $\frac{\partial E_{GWF}}{\partial g(\Gamma_i)}$ for a particular Γ_i does not involve the evaluation of other derivatives. Therefore, the computational workload of the approach can be easily handled by the efficient parallel computing.

The extension of GCGM method to more complex molecules or bulk materials is straightforward. Here, we use periodic bulk solids as an example to illustrate how to generalize the GCGM method to systems with more than 2 atoms. The Hamiltonian for a bulk system in the second quantization form can be expressed as,

$$H = \sum_{Ii\alpha,Jj\beta,\sigma} t_{Ii\alpha Jj\beta} c^{\dagger}_{Ii\alpha\sigma} c_{Jj\beta\sigma} + \frac{1}{2} \sum_{\substack{Ii\alpha,Jj\beta \\ Kk\gamma,Ll\delta,\sigma\sigma'}} u(Ii\alpha,Jj\beta;Kk\gamma,Ll\delta) c^{\dagger}_{Ii\alpha\sigma} c^{\dagger}_{Jj\beta\sigma'} c_{Ll\delta\sigma'} c_{Kk\gamma\sigma} \,, \tag{14}$$

where I,J,K,L represent the unit cell indices; i,j,k,l are the atomic site indices, $\alpha,\beta,\gamma,\delta$ the orbital indices, and σ,σ' the spin indices. The one-electron hopping integral, t, and the two-electron Coulomb integral, u, are defined similarly to Eq. (2)(3). The total energy is evaluated with the GWF of the form,

$$\left|\Psi_{GWF}\right\rangle = \prod_{Ii} \left(\sum_{\Gamma} g(\Gamma_{Ii}) \left|\Gamma_{Ii}\right\rangle \left\langle \Gamma_{Ii}\right| \right) \left|\Psi_0\right\rangle , \tag{15}$$

which is constructed from a non-interacting wave function $\left|\Psi_0\right\rangle$. $g(\Gamma_{Ii})$ is the Gutzwiller variational parameter determining the occupation probability of the on-site Fock state $\left|\Gamma_{Ii}\right\rangle$ at the atom site indexed "i" in the unit cell indexed "I". Since all unit cells are identical, $g(\Gamma_{Ii})$ does not depend on the specific unit cell and can be written as $g(\Gamma_{Ii}) = g(\Gamma_i)$. The total energy without adopting Gutzwiller approximation can be expressed as

$$\begin{aligned} E_{GWF} = & \sum_{Ii\alpha,Jj\beta,\sigma} t_{Ii\alpha,Jj\beta} \left\langle c^{\dagger}_{Ii\alpha\sigma} c_{Jj\beta\sigma} \right\rangle_{GWF} + \frac{1}{2} \sum_{\substack{I,i,\alpha\beta\gamma\delta \\ \sigma\sigma'}} u(Ii\alpha,Ii\beta;Ii\gamma,Ii\delta) \left\langle c^{\dagger}_{Ii\alpha\sigma} c^{\dagger}_{Ii\beta\sigma'} c_{Ii\delta\sigma'} c_{Ii\gamma\sigma} \right\rangle_{GWF} \\ & + \frac{1}{2} {\sum_{\substack{Ii\alpha,Jj\beta \\ Kk\gamma,Ll\delta,\sigma\sigma'}}}' \left(u(Ii\alpha,Jj\beta;Kk\gamma,Ll\delta) - \delta_{\sigma\sigma'} u(Ii\alpha,Jj\beta;Ll\delta,Kk\gamma) \right) \left\langle c^{\dagger}_{Ii\alpha\sigma} c_{Kk\gamma\sigma} \right\rangle_{GWF} \left\langle c^{\dagger}_{Jj\beta\sigma'} c_{Ll\delta\sigma'} \right\rangle_{GWF} \end{aligned} \tag{16}$$

where $\sum'$ indicates that the pure on-site terms are excluded from the summation. The on-site

2PCM are treated rigorously and the intersite 2PCM are evaluated using Wick's theorem. The 1PDM can be expressed as,[2]

$$\left\langle c^{\dagger}_{Ii\alpha\sigma} c_{Jj\beta\sigma} \right\rangle_{GWF} = \frac{1}{\left\langle \Psi_{GWF} \middle| \Psi_{GWF} \right\rangle_{Ii,Jj}} \sum_{\Gamma_{Ii},\Gamma_{Jj},\Gamma'_{Ii},\Gamma'_{Jj}} \left\langle \Gamma_{Ii} \middle| c^{\dagger}_{Ii\alpha\sigma} \middle| \Gamma'_{Ii} \right\rangle \left\langle \Gamma_{Jj} \middle| c_{Jj\beta\sigma} \middle| \Gamma'_{Jj} \right\rangle \cdot g(\Gamma_i) g(\Gamma_j) g(\Gamma'_i) g(\Gamma'_j) \xi_{\Gamma_{Ii},\Gamma_{Jj},\Gamma'_{Ii},\Gamma'_{Jj}} \tag{17}$$

where $\xi_{\Gamma_{Ii},\Gamma_{Jj},\Gamma'_{Ii},\Gamma_{Jj}}$ is coefficient determined from $\left|\Psi_0\right\rangle$ and Gutzwiller variational parameters $\{g(\Gamma_{Kk})\}, (K,k) \neq (I,i)\ or\ (J,j)$,

$$\xi_{\Gamma_{Ii},\Gamma_{Jj},\Gamma'_{Ii},\Gamma'_{Jj}} = \sum_{\{\Gamma_{Kk},Kk\neq Ii,Jj\}} \prod_{Kk} g(\Gamma_{Kk})^2 \left\langle \Psi_0 \middle| \Gamma_{Ii}, \Gamma_{Jj}, \{\Gamma_{Kk}\} \right\rangle \left\langle \Gamma'_{Ii}, \Gamma'_{Jj}, \{\Gamma_{Kk}\} \middle| \Psi_0 \right\rangle, \tag{18}$$

and

$$\left\langle \Psi_{GWF} \middle| \Psi_{GWF} \right\rangle_{Ii,Jj} = \sum_{\Gamma_{Ii},\Gamma_{Jj}} \xi_{\Gamma_{Ii},\Gamma_{Jj},\Gamma_{Ii},\Gamma_{Jj}} g(\Gamma_i)^2 g(\Gamma_j)^2 . \tag{19}$$

By comparing Eq. (17)-(19) with Eq. (10)-(12), one can find that the expression of 1PDM of a bulk system is very close to that of a diatomic molecule, except that the expression of ξ is different. Clearly, the computational time to rigorously evaluate the expectation values of an operator such as 1PDM (Eq.17), the norm of GWF (Eq.19), or equivalently the coefficient tensor ξ, grows exponentially with respect to the number of atomic sites, as the summation goes through all of them. Therefore, effective approximations to evaluate the coefficient tensor ξ has been adopted. As will be shown numerically, this approximation introduces some balanced errors

[2] For simplicity, Eq. (17) only presents 1PDM with $(I,i) \neq (J,j)$. The expressions of 1PDM with $(I,i) = (J,j)$ and the on-site 2PCM are very similar to the expressions in Eq. (9)(13) and are thus not presented here.

in the numerator and denominator when calculating the expectation value of operators such as density matrix, which ends up with quite good error cancellations. Furthermore, it guarantees that the method recovers the Hartree-Fock and atomic limits.

In the following we will take bulk Hydrogen as an example to illustrate how to approximate ξ in a simple way. For hydrogen systems described by minimal basis 1s-orbitals, there are 4 on-site Fock states at each H-atom: $|\varnothing\rangle, |\uparrow\rangle, |\downarrow\rangle, |\uparrow\downarrow\rangle$. And we have $g(|\varnothing\rangle) = g(|\uparrow\downarrow\rangle)$ since the orbital is half-filled. For simplicity, take $g(|\varnothing\rangle) = g(|\uparrow\downarrow\rangle) = g, g(|\uparrow\rangle) = g(|\downarrow\rangle) = 1$. The problem is to evaluate $\xi_{\Gamma_{Ii},\Gamma_{Jj},\Gamma'_{Ii},\Gamma'_{Jj}}$ in Eq. (18) concerning 2 sites *Ii*, *Jj* for large systems. Let us consider the case with $g \ll$, which implies the dominant onsite configuration is the singly occupied states. It corresponds to the system approaching dissociation limit. One can address the problem by considering the number of electrons $n_e(Ii), n_e(Jj)$ at the 2 sites. If $n_e(Ii) + n_e(Jj) = 2$, each of the rest sites will be occupied by 1 electron when a thermodynamic limit is approached, so $g(\Gamma_k) = 1$ in Eq. (18) as $\Gamma_k = |\uparrow\rangle \, or \, |\downarrow\rangle$. Eq. (18) thus becomes $\xi_{\Gamma_{Ii},\Gamma_{Jj},\Gamma'_{Ii},\Gamma'_{Jj}} = \langle\Psi_0|\Gamma_{Ii},\Gamma_{Jj}\rangle\langle\Gamma'_{Ii},\Gamma'_{Jj}|\Psi_0\rangle$. If $n_e(Ii) + n_e(Jj) = 1$, one electron must go to one of the rest sites and that site will be double occupied while all of other rest sites will be single occupied at the dissociation limit. So $\prod_{Kk\neq Ii,Jj} (g(\Gamma_k))^2 = (g(|\uparrow\downarrow\rangle))^2 (g(|\uparrow\rangle))^2 (g(|\uparrow\rangle))^2 ... (g(|\downarrow\rangle))^2 (g(|\downarrow\rangle))^2 ... = g^2 \cdot 1 \cdot 1 \cdot ... = g^2$ and Eq. (18) now becomes $\xi_{\Gamma_{Ii},\Gamma_{Jj},\Gamma'_{Ii},\Gamma'_{Jj}} = g^2 \langle\Psi_0|\Gamma_{Ii},\Gamma_{Jj}\rangle\langle\Gamma'_{Ii},\Gamma'_{Jj}|\Psi_0\rangle$. Similarly, if $n_e(Ii) + n_e(Jj) = 3$, one electron must go from one of the rest sites to site *Ii or Jj*. The site with the missing electron will be vacant and all other rest sites will be single occupied at thermodynamic limit. So

$\prod_{Kk\neq Ii,Jj}\left(g(\Gamma_k)\right)^2=\left(g(|\varnothing\rangle)\right)^2\left(g(|\uparrow\rangle)\right)^2\left(g(|\uparrow\rangle)\right)^2\ldots\left(g(|\downarrow\rangle)\right)^2\left(g(|\downarrow\rangle)\right)^2\ldots=g^2\cdot1\cdot1\cdot\ldots=g^2$, and Eq. (18) becomes $\xi_{\Gamma_{Ii},\Gamma_{Jj},\Gamma'_{Ii},\Gamma'_{Jj}}=g^2\langle\Psi_0|\Gamma_{Ii},\Gamma_{Jj}\rangle\langle\Gamma'_{Ii},\Gamma'_{Jj}|\Psi_0\rangle$. The expression to evaluate $\xi_{\Gamma_{Ii},\Gamma_{Jj},\Gamma'_{Ii},\Gamma'_{Jj}}$ is summarized in Eq. (20),

$$\xi_{\Gamma_{Ii},\Gamma_{Jj},\Gamma'_{Ii},\Gamma'_{Jj}}=\begin{cases}\xi^0_{\Gamma_{Ii},\Gamma_{Jj},\Gamma'_{Ii},\Gamma'_{Jj}}, \text{ if } n_e(Ii)+n_e(Jj)=2\\ g^2\xi^0_{\Gamma_{Ii},\Gamma_{Jj},\Gamma'_{Ii},\Gamma'_{Jj}}, \text{ if } n_e(Ii)+n_e(Jj)=1 \text{ or } 3\end{cases}, \tag{20}$$

where $\xi^0_{\Gamma_{Ii},\Gamma_{Jj},\Gamma'_{Ii},\Gamma'_{Jj}}$ is predetermined coefficient from $|\Psi_0\rangle$,

$$\xi^0_{\Gamma_{Ii},\Gamma_{Jj},\Gamma'_{Ii},\Gamma'_{Jj}}=\langle\Psi_0|\Gamma_{Ii},\Gamma_{Jj}\rangle\langle\Gamma'_{Ii},\Gamma'_{Jj}|\Psi_0\rangle. \tag{21}$$

We further point out that, although Eq. (21) is developed based on the assumption that the onsite singly occupied states are dominant, it also recovers the Hartree-Fock limit with uniform variational parameters.

For a general non-Hydrogen bulk system with n_e electrons/atom, Eq. (20) can be generalized to,

$$\xi_{\Gamma_{Ii},\Gamma_{Jj},\Gamma'_{Ii},\Gamma'_{Jj}}=\begin{cases}g^2_{(\Gamma^+)}\xi^0_{\Gamma_{Ii},\Gamma_{Jj},\Gamma'_{Ii},\Gamma'_{Jj}}, \text{ if } n_e(Ii)+n_e(Jj)=2n_e-1\\ \xi^0_{\Gamma_{Ii},\Gamma_{Jj},\Gamma'_{Ii},\Gamma'_{Jj}}, \text{ if } n_e(Ii)+n_e(Jj)=2n_e\\ g^2_{(\Gamma^-)}\xi^0_{\Gamma_{Ii},\Gamma_{Jj},\Gamma'_{Ii},\Gamma'_{Jj}}, \text{ if } n_e(Ii)+n_e(Jj)=2n_e+1\end{cases}, \tag{22}$$

where Γ^+ and Γ^- represent the dominant on-site configuration with 1 extra and 1 missing electron, respectively. In Eq. (22) we only consider 1 extra or missing electrons at sites *Ii*, *Jj*. Higher order approximations can be made if more than 1 extra or missing electrons are considered. Eq. (22) is a generalized approximation to effectively evaluate the coefficient tensor

$\xi_{\Gamma_{Ii},\Gamma_{Jj},\Gamma'_{Ii},\Gamma'_{Jj}}$. If we want to evaluate the 1PDM presented in Eq. (17) or the 2PCM, Eq. (22) should be used instead of Eq. (18) for evaluation of ξ in Eq. (17).

By comparing Eq. (11) and (21), one can see that $\xi^0_{\Gamma_{Ii},\Gamma_{Jj},\Gamma'_{Ii},\Gamma'_{Jj}}$ in Eq. (21) has the same form as $\xi^0_{\Gamma_i,\Gamma_j,\Gamma'_i,\Gamma'_j}$ in Eq. (11). They can be easily evaluated using the 1PDM of $|\Psi_0\rangle$ regarding sites Ii, Jj or sites i, j. Then $\xi_{\Gamma_{Ii},\Gamma_{Jj},\Gamma'_{Ii},\Gamma'_{Jj}}$ is readily evaluated from $\xi^0_{\Gamma_{Ii},\Gamma_{Jj},\Gamma'_{Ii},\Gamma'_{Jj}}$, as shown in Eq. (22). For a diatomic system, $n_e(Ii)+n_e(Jj)=2n_e$ is always true, and Eq. (22) gives $\xi_{\Gamma_{Ii},\Gamma_{Jj},\Gamma'_{Ii},\Gamma'_{Jj}} = \xi^0_{\Gamma_{Ii},\Gamma_{Jj},\Gamma'_{Ii},\Gamma'_{Jj}}$, thus the expression in Eq. (11) is recovered. So Eq. (22) can be regarded as a general expression of $\xi_{\Gamma_{Ii},\Gamma_{Jj},\Gamma'_{Ii},\Gamma'_{Jj}}$ that is compatible with both multi-atomic and diatomic systems.

3. RESULTS

Here we show the GCGM numerical results for N_2 dimer in spin-singlet ground state, as well as O_2 dimer in spin-triplet ground state. QUAsi-atomic Minimal Basis set Orbitals (QUAMBOs, see Ref. [51]) are used as basis-set orbitals (e.g. ϕ in Eq. (2) and (3)) with the $2s$ and $2p$ orbitals chosen as the on-site correlated orbitals. QUAMBOs are constructed from the aug-cc-pVTZ basis functions [52]. QUAMBO-based FCI, large basis CI results and experimental measurements are also presented for comparison. We also show the GCGM results for 1-dimensional hydrogen chain as an example of periodic bulk systems. The potential energy is evaluated using Eq. (5) for N_2, O_2 dimers and Eq. (16) for linear hydrogen chain.

3.1. N_2 dimer

N_2 is a popular example for strongly correlated systems and has been served as a benchmarking system with several theoretical methods [53]. Figure 1(a) shows the QUAMBO-based GCGM ground state total energy curve of N_2 in comparison with the results from QUAMBO-based FCI calculations. Remarkably, QUAMBO-GCGM produces energy curves in good agreement with the QUAMBO-FCI results (error in the binding energy is 0.0061 Hartrees, or 3.83 kcal/mol). The bound QUAMBO-CMR result is also included for comparison. The GCGM result is slightly better than CMR around the region of bond length $\sim$2 Å. More details on comparison of CMR and GCGM can be found in Discussion. To compare with experiment, dynamical correlation beyond the minimal basis calculations needs to be added. For simplicity, we adopt the local density approximation for the dynamical correlation energy E_c and evaluate it with PySCF package [54]. Figure 1. (b) plots the binding energy curve determined by GCGM+E_c and experiment [55,56] for comparison. GCGM+E_c produces energy curve in reasonable agreement with experiment (error in the binding energy is 0.016 Hartrees, or 10.0 kcal/mol), illustrating the correct recipe to include E_c in the total energy.

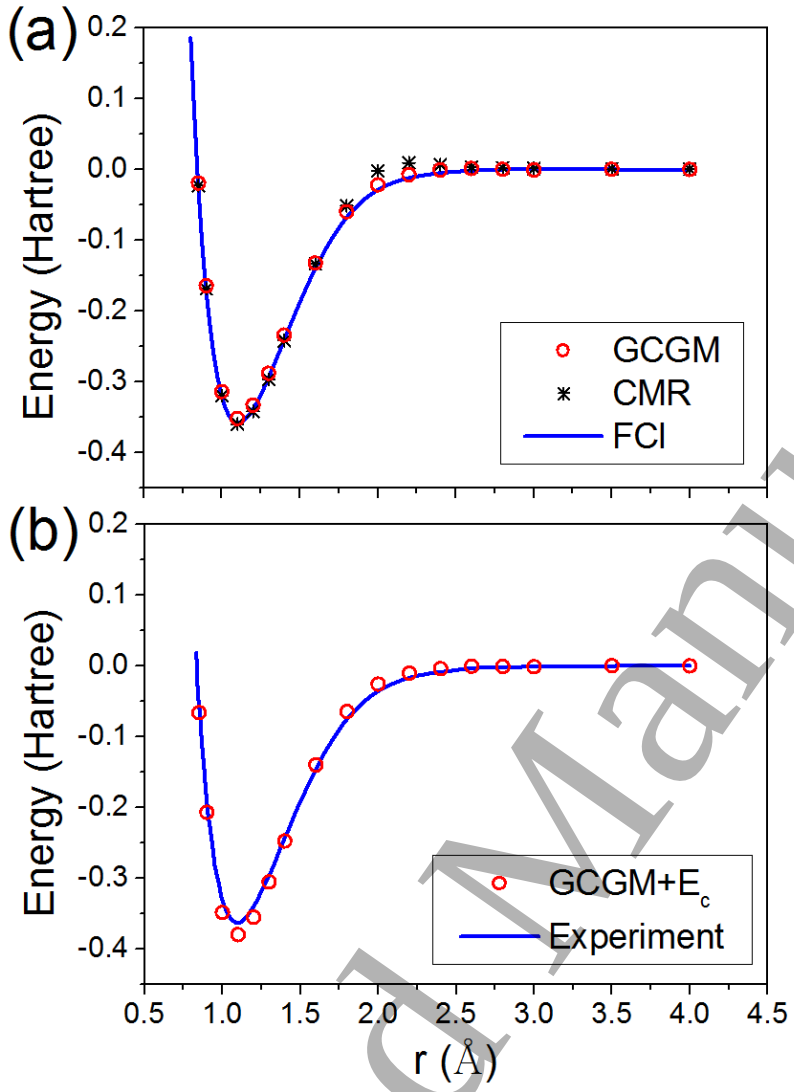

Figure 1. Potential energy curves of N_2 determined by (a) GCGM, CMR and FCI methods, and (b) GCGM+E_c and experiments [54,55]. The GCGM, CMR and FCI calculations are based on QUAMBOs constructed from the aug-cc-pVTZ basis set.

3.2. O_2 dimer

Here, we use O_2 dimer as an example to show that GCGM also promotes more flexibility within Gutzwiller framework. We study the potential energy curve for both the ground state $X^3\Sigma_g^-$, or 'triplet oxygen', and the lowest excited state $a^1\Delta_g$, or 'singlet oxygen'. Figure 2(a)

shows the QUAMBO-GCGM potential energy curve in comparison with QUAMBO-FCI for the singlet and triplet states. GCGM produces energy curves in close agreement with QUAMBO-FCI for the singlet state (the binding energy error is 0.0035 Hartrees, or 2.20 kcal/mol) and at the bound region for the triplet state. However, GCGM yields surprisingly wrong results at the atomic limit for the triplet state.

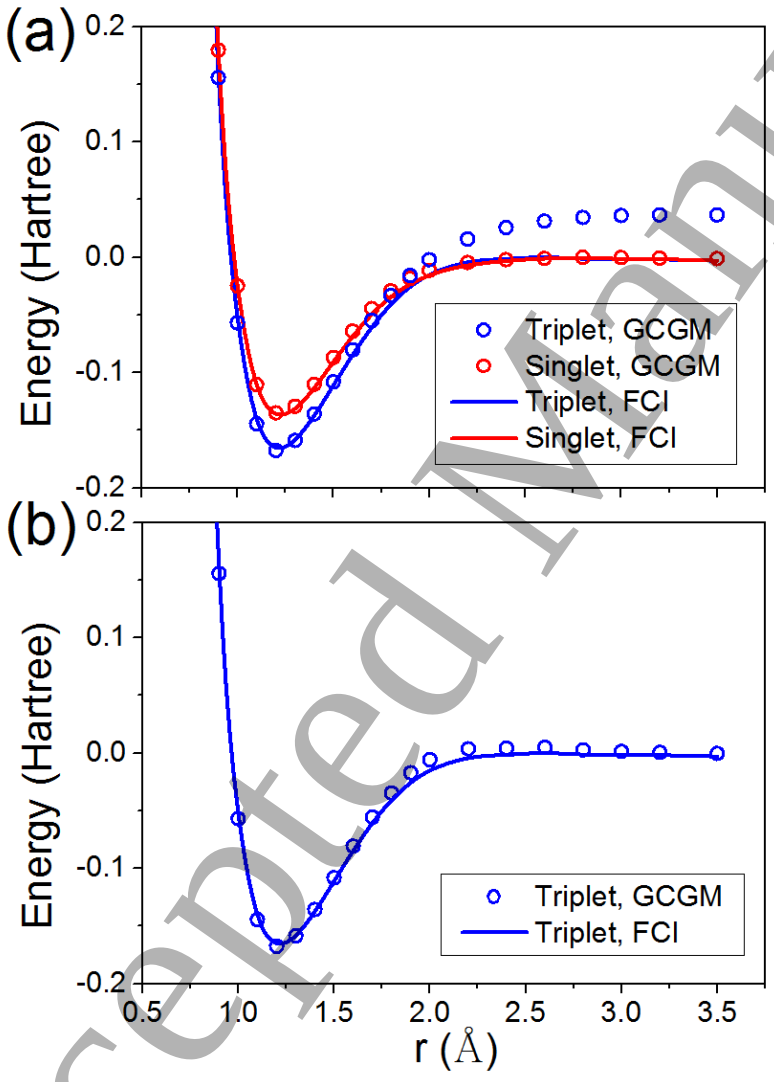

Figure 2. Potential energy curves of O2 determined by (a) GCGM and FCI methods, where the atomic limit of GCGM is wrong for the ground triplet $X^3\Sigma_g^-$ state; and (b) the corrected GCGM

and FCI methods for $X^3\Sigma_g^-$, where the atomic limit solution is included in the trial wave function in GCGM. The GCGM and FCI calculations are based on QUAMBOs constructed from the aug-cc-pVTZ basis set.

After a careful investigation of the atomic limit solution, we found that the reason for the discrepancy is that the non-interacting wave function $|\Psi_0\rangle$, from which the Gutzwiller wave function is constructed, does not contain the configurations of the atomic limit solution. The triplet $X^3\Sigma_g^-$ state has $S = 1$. If it can be described with a single Slater determinant $|\Psi_0\rangle$, S_z can only be either 1 or -1. We picked $S_z = 1$ for demonstration. When the two oxygen atoms pull away from each other towards the atomic limit, both atoms must have $S_z = 1/2$ from symmetry of $|\Psi_0\rangle$ and spin conservation, which is not the atomic solution (oxygen atom has $S_z = -1, 0\ or\ 1$). So $|\Psi_0\rangle$ cannot contain the configurations of the atomic limit solution.

To address this problem, we need to introduce some mechanism to feed in the atomic solutions. One possible way is to use the GWF with Gutzwiller correlator expressed in terms of atomic eigen-states, or in its rotationally invariant form [57-59]. However, it will significantly increase the complexity of the formalism and computational time. Alternatively, we here included the atomic limit solution straightforwardly in the trial wave function,

$$|\Psi_0'\rangle = |\Psi_0\rangle + \lambda|\Psi_a\rangle \tag{23}$$

where $|\Psi_a\rangle$ is the atomic limit solution, and λ is the factor determing the weight of $|\Psi_a\rangle$. $|\Psi_a\rangle$ is set to let one oxygen atom has $S = 1, S_z = 1$ and the other atom has $S = 1, S_z = 0$. Then the total energy is minimized with respect to both $\{g(\Gamma_i)\}$ and λ. Fig. 2(b) plots the corrected GCGM

energy in comparison with QUAMBO-FCI for triplet oxygen and good agreement is achieved (the binding energy error is 0.0023 Hartrees, or 1.44 kcal/mol). Fig. 3 plots the binding energy curve of GCGM+E_c and the large basis CI [60] for comparison, where close agreement is established again (the binding energy error is 0.0022 and 0.0027 Hartrees for singlet and triplet, respectively).

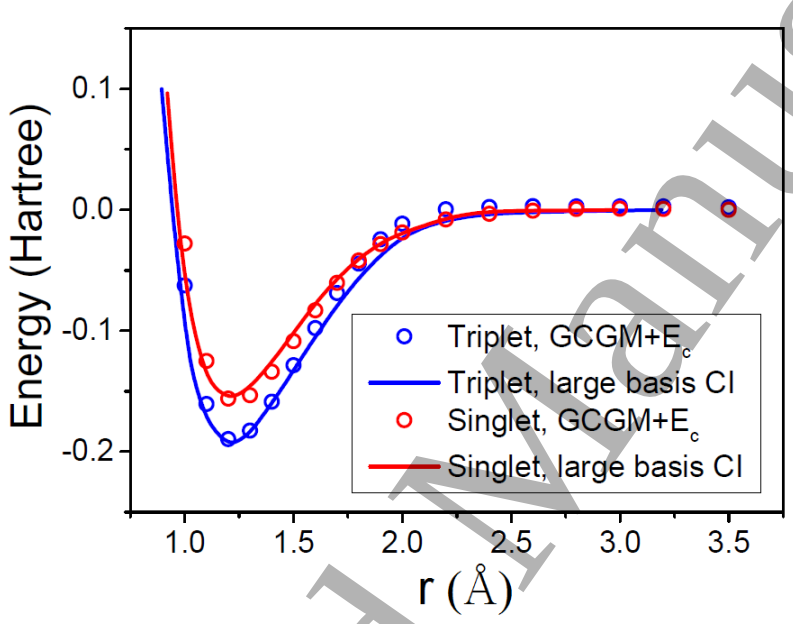

Figure 3. Potential energy curves of triplet and singlet oxygen with GCGM+E_c and large basis CI [60] for comparison.

3.3. 1-D hydrogen chain

We benchmark the accuracy of our GCGM method for periodic bulk systems using one-dimensional chain of hydrogen atoms. The linear hydrogen chain is the simplest periodic system, yet it is an ideal first benchmark system for testing the ability of many-body methods to treat correlation effects [61]. It also serves as a testing base to benchmark the compuational efficiency of these methods. On one hand, the full Coulomb interaction needs to be treated for accurate

description for electron correlations of this system. On the other hand, the hydrogen chain does not have the complexities of treating core electrons or incorporating relativistic effects. Therefore, many theoretical methods can be benchmarked with hydrogen chain, as discussed in details in the recent work [61].

As shown in Fig. 4, the potential energy curve as a function of interatomic distance from our GCGM calculations is compared with the one using auxiliary-field quantum Monte Carlo (AFQMC) reported in Ref. [61]. The results from density functional calculations with local density approximation (LDA) and the Hartree Fock (HF) method are also plotted for comparison. In our GCGM calculation, 22 k-points are used, or equivalently, 22 atomic sites with periodic boundary condition. From Fig. 4, one can see that a good agreement between GCGM and AFQMC results is achieved with a binding energy error of 0.022 eV/atom and that GCGM performs much better than the standard LDA or HF, especially when the interatomic distance gets larger. One downside of some popular theoretical methods to deal with correlated-electron systems is that their computational load increases dramatically as the system size gets bigger. Although they can be very accurate describing small systems, their power are restricted for big molecules or bulk materials. The GCGM method is developed with the motivation that a good balance between accuracy and computational efficiency can be achieved. As we will show in DISCUSSION later, GCGM scales a little more than linearly with system size for periodic systems, indicating a promising computational efficiency while maintaining satisfying accuracy.

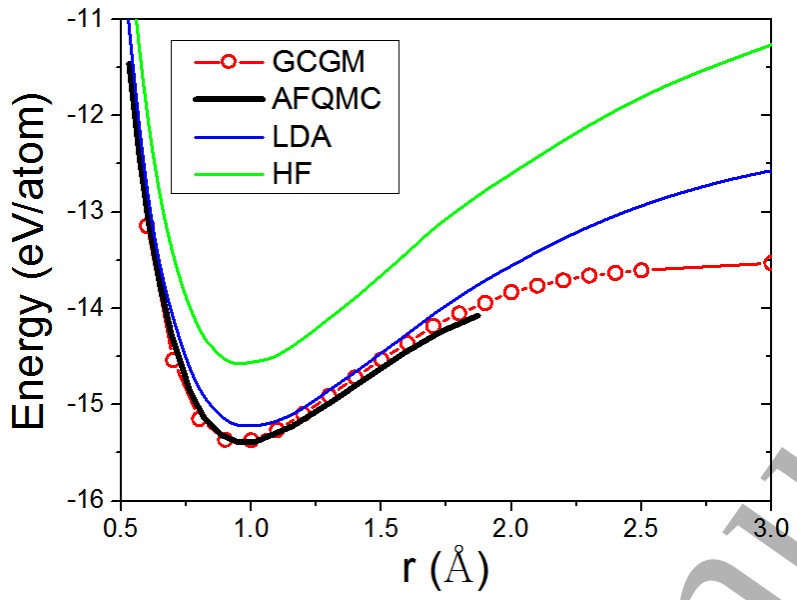

Figure 4. Potential energy curves of one-dimensional hydrogen chain calculated from different methods as indicated.

4. DISCUSSION

The example of triplet oxygen $X^3\Sigma_g^-$ demonstrates the important role that the non-interacting wave function $|\Psi_0\rangle$ plays in the Gutzwiller framework. An accurate solution cannot be obtained if $|\Psi_0\rangle$ does not contain certain configurations which are present in the real solution. It is worth noting that in our GCGM approach, $|\Psi_0\rangle$ can be easily modified to accommodate all possible configurations like the multireference configuration interaction method does. In the example of triplet oxygen, $|\Psi_0\rangle$ is mixed with the atomic solution to get the accurate solution at the atomic limit. To study the constraint from $|\Psi_0\rangle$ in the Gutzwiller scheme, we compare the GWF and the FCI wave function in the following.

For a finite system with N sites, the exact ground state many-body wave function, i.e., the FCI wave function, is a vector in the Fock space of the following form

$$\left|\Psi_{FCI}\right\rangle = \sum_{\{\Gamma_1,\Gamma_2,...,\Gamma_N\}} \lambda(\Gamma_1\Gamma_2...\Gamma_N)\left|\Gamma_1\Gamma_2...\Gamma_N\right\rangle, \tag{24}$$

where Γ_i is the on-site Fock state at site i. The GWF in Eq. (4) can be rewritten as

$$\left|\Psi_{GWF}\right\rangle = \sum_{\{\Gamma_1,\Gamma_2,...,\Gamma_N\}} g(\Gamma_1)g(\Gamma_2)...g(\Gamma_N)\left|\Gamma_1\Gamma_2...\Gamma_N\right\rangle\left\langle\Gamma_1\Gamma_2...\Gamma_N\middle|\Psi_0\right\rangle, \tag{25}$$

Clearly, the GWF represents an approximation to the FCI wave function by taking the linear expansion coefficient λ in the form of

$$\lambda(\Gamma_1\Gamma_2...\Gamma_N) = g(\Gamma_1)g(\Gamma_2)...g(\Gamma_N)\left\langle\Gamma_1\Gamma_2...\Gamma_N\middle|\Psi_0\right\rangle. \tag{26}$$

It contains a simple site-wise product of g-factors with site correlations encoded in $\left|\Psi_0\right\rangle$. It is interesting to check the impact of the factorization of λ as in the GWF and its dependence on $\left|\Psi_0\right\rangle$. A parameter Δ is introduced to control the dependence of $\left|\Psi_{GWF}\right\rangle$ on $\left|\Psi_0\right\rangle$. We change the coefficient $\left\langle\Gamma_1\Gamma_2...\Gamma_N\middle|\Psi_0\right\rangle$ in Eq. (25) to be,

$$\left\langle\Gamma_1\Gamma_2...\Gamma_N\middle|\Psi_0\right\rangle = \begin{cases} \left\langle\Gamma_1\Gamma_2...\Gamma_N\middle|\Psi_0\right\rangle, & when \left|\left\langle\Gamma_1\Gamma_2...\Gamma_N\middle|\Psi_0\right\rangle\right| \geq \Delta \\ \Delta, & when \left|\left\langle\Gamma_1\Gamma_2...\Gamma_N\middle|\Psi_0\right\rangle\right| < \Delta \end{cases} \tag{27}$$

So the minimum of $\left|\left\langle\Gamma_1\Gamma_2...\Gamma_N\middle|\Psi_0\right\rangle\right|$ is set to be the adjustable Δ. $\left|\left\langle\Gamma_1\Gamma_2...\Gamma_N\middle|\Psi_0\right\rangle\right|$ is a number between 0 and 1 for a normalized $\left|\Psi_0\right\rangle$. By adjusting Δ, one can control the dependence of $\left|\Psi_{GWF}\right\rangle$ on $\left|\Psi_0\right\rangle$. For $\Delta = 0$, the original GCGM results are exactly reproduced. As Δ gets larger, $\left|\Psi_{GWF}\right\rangle$ gradually loses the dependence on $\left|\Psi_0\right\rangle$ and configurations which are not present

in $|\Psi_0\rangle$ begin to come into play. For $\Delta = 1$, the dependence of $|\Psi_{GWF}\rangle$ on $|\Psi_0\rangle$ is fully removed and $\lambda(\Gamma_1\Gamma_2...\Gamma_N)$ in Eq. (26) is exclusively factorized by $g(\Gamma_i)$.

The triplet oxygen $X^3\Sigma_g^-$ is picked again as a prototypical case that the configurations of the real solution are absent in $|\Psi_0\rangle$ at certain bond length. In Fig. 5 we plot the energy curve of $X^3\Sigma_g^-$ with $\Delta = 0, 0.01, 1$ in comparison with QUAMBO-FCI. $\Delta = 0$ just replicates the energy curve as shown in Fig. 2(a). As mentioned earlier, GCGM yields wrong results at the atomic limit because $|\Psi_0\rangle$ does not contain the configurations of the atomic solution. By setting $\Delta = 1$, one includes all possible configurations which are not included in $|\Psi_0\rangle$ by eliminating the dependence of $|\Psi_{GWF}\rangle$ on $|\Psi_0\rangle$. The GCGM yields correct results at the atomic limit. However, the energy is too high at the bonding region, illustrating the importance of $|\Psi_0\rangle$ and the effectiveness of the GWF scheme. It can be seen that $\Delta = 0$ and 1 produce the correct energies at the bound region and the dissociation limit, respectively. At the intermediate region, e.g. $r \sim 2$Å, a Δ is to be selected to help one solution transit to the other smoothly. Here, we choose $\Delta = 0.01$. One can nearly reproduce the FCI results by selecting the minimum of the 3 GCGM energies with $\Delta = 0, 0.01, 1$ at each bond length. In principle, one needs to scan Δ ranging from 0 to 1 and get the minimum energy. From our experience, it suffices to pick up several values of Δ, for example, 0, 0.01, 1, calculate the energies with these Δs, and choose the minimal one. $\Delta = 0.01$ may not be the best selection at the intermediate region. However, choosing other Δ does not raise a significant improvement in energy. For example, if we choose $\Delta = 0, 0.02, 1$ instead of $\Delta = 0, 0.01, 1$, the resulting change in energy is only ~ 0.002 Hartree.

Eq. (23) and Eq.(27) provide 2 alternative ways to include configurations that are not originally included in $|\Psi_0\rangle$. If one knows what are relevent configurations to include, Eq. (23) can be used to include these configurations straightforwardly, where λ determines the weight of the configurations. However, if one has no information on what configurations should be included, Eq. (27) can be used to include all possible configurations by giving them a minimum weight measured by Δ. We note that there is no direct relationship between λ and Δ.

Our study clearly demonstrates the importance of $|\Psi_0\rangle$ in the Gutzwiller framework. At the same time, the limitation of the Gutzwiller scheme from $|\Psi_0\rangle$ is also shown. Fortunately, the limitation can be overcomed in our GCGM approach by modifying $|\Psi_0\rangle$ to accommodate all possible configurations. From variational minimization point of view, both the reference wavefunction $|\Psi_0\rangle$ and Gutzwiller projector should be simultaneously optimized. Indeed, in some variational quantum Monte Carlo approaches where the variational wavefunction is of Jastrow-Slater and Jastrow-antisymmetric geminal power (AGP) ansatz, both fermionic and Jastrow part are fully optimized within the given parameterized function form [62-64]. In the current GCGM calculations, the $|\Psi_0\rangle$ is first fixed to be the restricted HF or restricted open-shell HF wavefunction of the corresponding spin-multiplicity for simplicity. The reported modification of $|\Psi_0\rangle$ by adding the atomic wavefunction or minor tuning of the missing atomic configurations represents a simple and yet quite effective way to improve the ground state solutions when approaching the atomic limits.

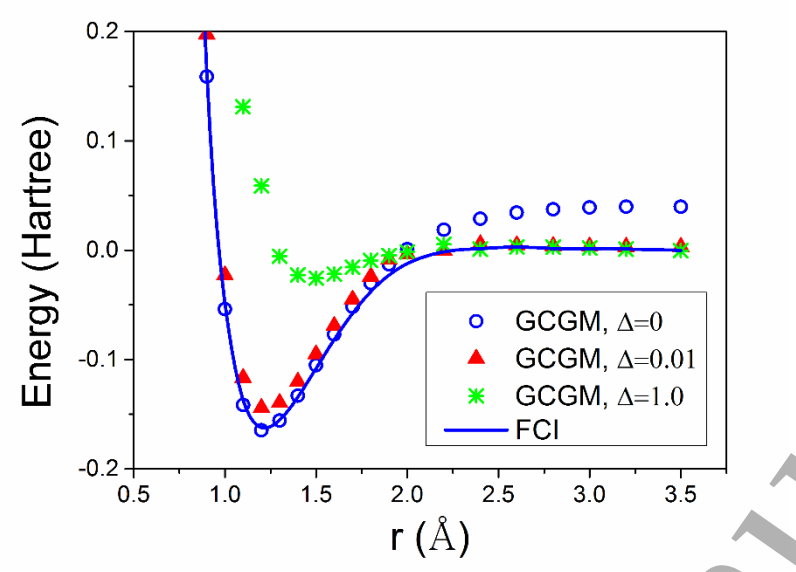

Figure 5. Potential energy curves of the triplet oxygen $X^3\Sigma_g^-$ using GCGM with $\Delta = 0, 0.01, 1$ and FCI methods.

In the CMR approach proposed in our previous work [49], a modified Gutzwiller approximation is applied and the single-electron term can be written as,

$$\left\langle c_{i\alpha\sigma}^{\dagger} c_{j\beta\sigma} \right\rangle_{CMR} \approx z_{i\alpha\sigma}^{j\beta} \left\langle c_{i\alpha\sigma}^{\dagger} c_{j\beta\sigma} \right\rangle_0, \tag{28}$$

where $z_{i\alpha\sigma}^{j\beta} = \sqrt{z_{i\alpha\sigma}^{GA} z_{j\beta\sigma}^{GA}}$ if $(i\alpha) \neq (j\beta)$ and 1 otherwise. The z factor can be evaluated as,

$$z_{i\alpha\sigma}^{GA} = \sum_{\Gamma\Gamma'} \frac{\sqrt{p_{i\Gamma} p_{i\Gamma'}} \left| \left\langle \Gamma_i \left| c_{i\alpha\sigma}^{\dagger} \right| \Gamma_i' \right\rangle \right|}{\sqrt{n_{i\alpha\sigma}^0 (1 - n_{i\alpha\sigma}^0)}}. \tag{29}$$

Here, $n_{i\alpha\sigma}^0 = \left\langle c_{i\alpha\sigma}^{\dagger} c_{i\alpha\sigma} \right\rangle_0 = \left\langle \Psi_0 \left| c_{i\alpha\sigma}^{\dagger} c_{i\alpha\sigma} \right| \Psi_0 \right\rangle$, and $p_{i\Gamma}$ is the Fock state occupation probability. The modified orbital renormalization form is obtained by comparison with the exact analytical total energy expression of the minimal basis hydrogen dimer. In the GCGM approach presented in this work, the equivalent $z_{i\alpha\sigma}^{j\beta}$ can be written as from Eq. (10),

$$z_{i\alpha\sigma}^{j\beta} = \frac{\sum_{\Gamma_i,\Gamma_j,\Gamma'_i,\Gamma'_j} \langle \Gamma_i | c_{i\alpha\sigma}^{\dagger} | \Gamma'_i \rangle \langle \Gamma_j | c_{j\beta\sigma} | \Gamma'_j \rangle g(\Gamma_i) g(\Gamma_j) g(\Gamma'_i) g(\Gamma'_j) \xi_{\Gamma_i,\Gamma_j,\Gamma'_i,\Gamma'_j}}{\sum_{\Gamma_i,\Gamma_j,\Gamma'_i,\Gamma'_j} \langle \Gamma_i | c_{i\alpha\sigma}^{\dagger} | \Gamma'_i \rangle \langle \Gamma_j | c_{j\beta\sigma} | \Gamma'_j \rangle \xi_{\Gamma_i,\Gamma_j,\Gamma'_i,\Gamma'_j}}, \quad (30)$$

if $i \neq j$ (the formalism for $i = j$ is not presented here for conciseness). Comparing Eq. (28) and (30), it can be seen that the GCGM approach is different from CMR by NOT factorizing the z factor. The GCGM approach also features improved flexibility in selecting $|\Psi_0\rangle$ discussed above. As shown in the example of O_2, $|\Psi_0\rangle$ can be modified to accommodate all possible configurations to give an accurate solution at atomic limit. On the other hand, since CMR is based on Gutzwiller approximation and Gutzwiller framework that the GWF is constructed on the basis of the single Slater determinant $|\Psi_0\rangle$, such extension of $|\Psi_0\rangle$ is not as straightforward as in GCGM and still needs extra exploration.

Finally, we want to discuss the scaling of our GCGM method with a system of increasing size. We consider a N-site(atom) system. From Eq. (16), one needs to evaluate the 1PDM $\langle c_{Ii\alpha\sigma}^{\dagger} c_{Jj\beta\sigma} \rangle_{GWF}$ and on-site 2PCM $\langle c_{Ii\alpha\sigma}^{\dagger} c_{Ij\beta\sigma}^{\dagger} c_{Ii\delta\sigma'} c_{Ii\gamma\sigma} \rangle_{GWF}$ to calculate the total energy. The number of on-site 2PCM terms to be evaluated is N. The number of 1PDM terms is the number of pairs of atoms to be considered in the system, i.e. $N-1$ for periodic bulk systems or $N(N-1)/2$ for molecules. Thus, we expect our GCGM method scales linearly with system size for periodic bulk systems and quadratically for molecules. In Fig. 6, we test the scaling of our GCGM method with 1-D hydrogen chain. We plot the computation time against the number of k-points, or equivalently, number of atoms with periodic boundary condition. One can see that GCGM method scales a little more than linearly with system size. This is because that a small

fraction of computation time is attributed to the calculation of Fock terms which scales $\sim N^4$, as our method adopts Hartree-Fock-type factorization for the intersite two-body interactions.

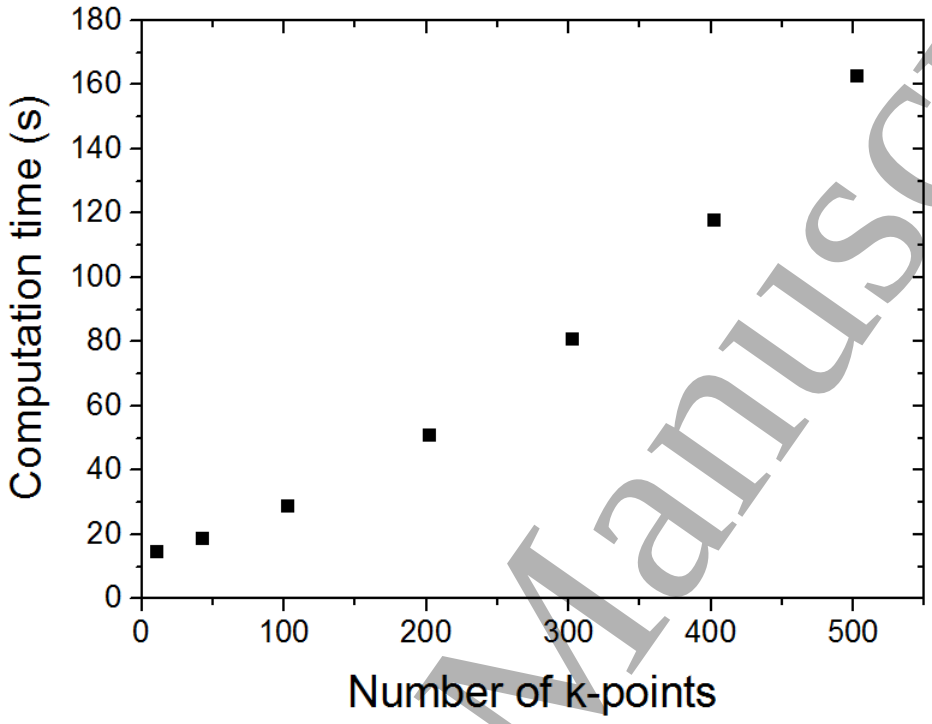

Figure 6. Computation time (using 1 core) against the number of k-points for 1-D hydrogen chain at interatomic distance of 1 Å.

5. CONCLUSION

To go beyond some intrinsic limitations of Gutzwiller approximation and boost the accuracy, we propose a method, namely GCGM, that bypasses Gutzwiller approximation for energy calculation of correlated electron systems. The total energy can be expressed explicitly as a function of Gutzwiller variational parameters and minimized with conjugate gradient method. GCGM is benchmarked by calculating the binding energy curves of N_2 and O_2 dimers, which are selected as benchmark cases for non-magnetic and magnetic systems, respectively. One-

dimensional hydrogen chain is also selected as a prototype periodic bulk system that goes much beyond diatomic molecules. The method produces energy curves in good agreement with QUAMBO-FCI, experiment data, large basis CI or AFQMC results. The method also features ideal parallel efficiency, which relieves the extra computational burden without resorting to Gutzwiller approximation. The dependence of Gutzwiller wave function on the trial non-interacting wave function is also discussed. We showed that the GCGM method adds more freedom in treating the trial wave function to achieve more accurate description of correlated electron materials.

ACKNOWLEDGMENTS

This work was supported by the U.S. Department of Energy (DOE), Office of Science, Basic Energy Sciences, Materials Science and Engineering Division, including the computer time support from the National Energy Research Scientific Computing Center (NERSC) in Berkeley, CA. The research was performed at Ames Laboratory, which is operated for the U.S. DOE by Iowa State University under Contract No. DEAC02-07CH11358. KMH were also partially supported by the China USTC Qian-Ren B (1000-Talents Program B) fund.

REFERENCES

[1] Hohenberg P and Kohn W 1964 Inhomogeneous Electron Gas *Phys. Rev.* **136** B864−B871

[2] Kohn W and Sham L 1965 Self-Consistent Equations Including Exchange and Correlation Effects *J. Phys. Rev.* **140** A1133−A1138

[3] Roos B O, Lindh R, Malmqvist P Å, Veryazov V and Widmark P O 2016 Multiconfigurational Quantum Chemistry (John Wiley & Sons)

[4] Roos B O, Taylor P R and Siegbahn P E M 1980 A Complete Active Space SCF Method (CASSCF) Using a Density Matrix Formulated Super-CI Approach *Chem. Phys.* **48** 157-173

[5] Cheung L M, Sundberg K R and Ruedenberg K 1978 Dimerization of Carbene to Ethylene *J. Am. Chem. Soc.* **100** 8024-8025

[6] Ruedenberg K, Schmidt M W, Gilbert M M and Elbert S T 1982 Are Atoms Intrinsic to Molecular Electronic Wavefunctions? I. The FORS Model *Chem. Phys.* **71** 41-49

[7] Olsen J, Roos B O, Jorgensen P and Jensen H J A 1988 Determinant based Configuration Interaction Algorithms for Complete and Restricted Configuration Interaction Spaces *J. Chem. Phys.* **89** 2185-2192

[8] Malmqvist P A, Rendell A and Roos B O 1990 The Restricted Active Space Self-Consistent-Field Method, Implemented with a Split Graph Unitary Group Approach *J. Phys. Chem.* **94** 5477-5482

[9] White S R 1992 Density Matrix Formulation for Quantum Renormalization Groups *Phys. Rev. Lett.* **69** 2863-2866

[10] Schollwöck U 2011 The Density-Matrix Renormalization Group in the Age of Matrix Product States *Ann. Phys.* **326** 96-192

[11] White S R and Feiguin A E 2004 Real-Time Evolution Using the Density Matrix Renormalization Group *Phys. Rev. Lett.* **93** 076401

[12] Zheng H and Wagner L K 2015 Computation of the Correlated Metal-Insulator Transition in Vanadium Dioxide from First Principles *Phys. Rev. Lett.* **114** 176401

[13] Ma F, Purwanto W, Zhang S and Krakauer H 2015 Quantum Monte Carlo Calculations in Solids with Downfolded Hamiltonians. *Phys. Rev. Lett.* **114** 226401

[14] Devaux N, Casula M, Decremps F and Sorella S 2015 Electronic Origin of the Volume Collapse in Cerium *Phys. Rev. B* **91** 081101

[15] Anisimov V I, Zaanen J and Andersen O K 1991 Band theory and Mott insulators: Hubbard U instead of Stoner I *Phys. Rev. B* **44** 943−954

[16] Anisimov V I, Aryasetiawan F and Lichtenstein I 1997 First-Principles Calculations of the Electronic Structure and Spectra of Strongly Correlated Systems: the LDA+ U Method *J. Phys.:Condens. Matter* **9** 767−808

[17] Georges A, Kotliar G, Krauth W and Rozenberg M J 1996 Dynamical Mean-Field Theory of Strongly Correlated Fermion Systems and the Limit of Infinite Dimensions *Rev. Mod. Phys.* **68** 13−125

[18] Savrasov S Y, Kotliar G and Abrahams E 2001 Correlated Electrons in δ-Plutonium within a Dynamical Mean-field Picture *Nature* **410** 793−795

[19] Kotliar G, Savrasov S Y, Haule K, Oudovenko V S, Parcollet O and Marianetti C A 2006 Electronic Structure Calculations with Dynamical Mean-Field Theory *Rev. Mod. Phys.* **78** 865−951

[20] Ho K M, Schmalian J and Wang C Z 2008 Gutzwiller Density Functional Theory for Correlated Electron Systems *Phys. Rev. B* **77** 073101

[21] Yao Y X, Wang C Z and Ho K M 2011 Including Many-Body Screening into Self-Consistent Calculations: Tight-Binding Model Studies with the Gutzwiller Approximation *Phys. Rev. B* **83** 245139

[22] Deng X Y, Wang L, Dai X and Fang Z 2009 Local Density Approximation Combined with Gutzwiller Method for Correlated Electron Systems: Formalism and Applications *Phys. Rev. B* **79** 075114

[23] Lanatà N, Strand H U R, Dai X and Hellsing B 2012 Efficient Implementation of the Gutzwiller Variational Method *Phys. Rev. B* **85** 035133

[24] Wang G, Qian Y, Xu G, Dai X and Fang Z 2010 Gutzwiller Density Functional Studies of FeAs-Based Superconductors: Structure Optimization and Evidence for a Three-Dimensional Fermi Surface *Phys. Rev. Lett.* **104** 047002

[25] Gutzwiller M C 1963 Effect of Correlation on the Ferromagnetism of Transition Metals *Phys. Rev. Lett.* **10** 159-162

[26] Gutzwiller M C 1964 Effect of Correlation on the Ferromagnetism of Transition Metals *Phys. Rev.* **134** A923

[27] Gutzwiller M C 1965 Correlation of Electrons in a Narrow S Band *Phys. Rev.* **137** A1726

[28] Brinkman W F and Rice T M 1970 Application of Gutzwiller's Variational Method to the Metal-Insulator Transition *Phys. Rev. B* **2** 4302-4304

[29] Florêncio J and Chao K A 1975 Antiferromagnetic Ground State in the S-Band Hubbard Model *Phys. Rev. Lett.* **35** 741-744

[30] Yao Y X, Schmalian J, Wang C Z, Ho K M and Kotliar G 2011 Comparative Study of the Electronic and Magnetic Properties of $BaFe_2As_2$ and $BaMn_2As_2$ Using the Gutzwiller Approximation *Phys. Rev. B* **84** 245112

[31] Lu F, Zhao J, Weng H, Fang Z and Dai X 2013 Correlated Topological Insulators with Mixed Valence *Phys. Rev. Lett.* **110** 096401

[32] Jastrow R 1955 Many-Body Problem with Strong Forces *Phys. Rev.* **98** 1479-1484

[33] Umrigar C J, Wilson K G, Wilkins J W 1988 Optimized Trial Wave Functions for Quantum Monte Carlo Calculations *Phys. Rev. Lett.* **60** 1719-1722

[34] Schmidt K E and Moskowitz J W 1990 Correlated Monte Carlo Wave Functions for the Atoms He Through Ne *J. Chem. Phys.* **93** 4172-4178

[35] Mitáš L and Martin R M 1994 Quantum Monte Carlo of Nitrogen: Atom, Dimer, Atomic, and Molecular Solids *Phys. Rev. Lett.* **72** 2438-2441

[36] Williamson A J, Kenny S D, Rajagopal G, James A J, Needs R J, Fraser L M, Foulkes W M C and Maccullum P 1996 Optimized Wave Functions for Quantum Monte Carlo Studies of Atoms and Solids *Phys. Rev. B* **53** 9640-9648

[37] Ogawa T, Kanda K and Matsubara T 1975 Gutzwiller Approximation for Antiferromagnetism in Hubbard Model *Prog. Theor. Phys.* **53** 614-633

[38] Kotliar G and Ruckenstein A E 1986 New Functional Integral Approach to Strongly Correlated Fermi Systems: The Gutzwiller Approximation as a Saddle Point *Phys. Rev. Lett.* **57** 1362-1365

[39] Bünemann J and Gebhard F 2007 Equivalence of Gutzwiller and Slave-Boson Mean-Field Theories for Multiband Hubbard Models *Phys. Rev. B* **76** 193104

[40] Vollhardt D 1984 Normal ^{3}He: an Almost Localized Fermi Liquid *Rev. Mod. Phys.* **56** 99-120

[41] Bünemann J and Weber W 1997 Generalized Gutzwiller Method for n⩾2 Correlated Bands: First-Order Metal-Insulator Transitions *Phys. Rev. B* **55** 4011-4014

[42] Fabrizio M 2007 Gutzwiller Description of Non-Magnetic Mott Insulators: Dimer Lattice Model *Phys. Rev. B* **76** 165110

[43] Gebhard F and Vollhardt D 1987 Correlation Functions for Hubbard-Type Models: The Exact Results for the Gutzwiller Wave Function in One Dimension *Phys. Rev. Lett.* **59** 1472-1475

[44] Metzner W and Vollhardt D 1987 Ground-State Properties of Correlated Fermions: Exact Analytic Results for the Gutzwiller Wave Function *Phys. Rev. Lett.* **59** 121-124

[45] Gebhard F 1990 Gutzwiller Correlated Wave Functions in Finite Dimensions d: A Systematic Expansion in 1/d *Phys. Rev. B* **41** 9452-9473

[46] Bünemann J, Schickling T and Gebhard F 2012 Variational Study of Fermi Surface Deformations in Hubbard Models *Europhys. Lett.* **98** 27006

[47] Yao Y X, Liu J, Wang C Z and Ho K M 2014 Correlation Matrix Renormalization Approximation for Total-Energy Calculations of Correlated Electron Systems *Phys. Rev. B* **89** 045131

[48] Yao Y X, Liu J, Liu C, Lu W C, Wang C Z and Ho K M 2015 Efficient and Accurate Treatment of Electron Correlations with Correlation Matrix Renormalization Theory *Sci. Rep.* **5** 13478

[49] Liu C, Liu J, Yao Y X, Wu P, Wang C Z and Ho K M 2016 Correlation Matrix Renormalization Theory: Improving Accuracy with Two-Electron Density-Matrix Sum Rules *J. Chem. Theory Comput.* **12** 4806-4811

[50] Wick G C 1950 The Evaluation of the Collision Matrix *Phys. Rev.* **80** 268-272

[51] Lu W C, Wang C Z, Schmidt M W, Bytautas L, Ho K M and Ruedenberg K J 2004 Molecule Intrinsic Minimal Basis Sets. I. Exact Resolution of Ab Initio Optimized Molecular Orbitals in Terms of Deformed Atomic Minimal-Basis Orbitals *J. Chem. Phys.* **120** 2629-2637

[52] Dunning T H 1989 Gaussian Basis Sets for Use in Correlated Molecular Calculations. I. The

Atoms Boron Through Neon and Hydrogen *J. Chem. Phys.* **90** 1007

[53] Stemmle C, Paulus B and Legeza Ö Analysis of electron-correlation effects in strongly correlated systems (N_2 and N_2^+) by applying the density-matrix renormalization-group method and quantum information theory *Phys. Rev. A* **97**, 022505

[54] Sun Q *et al.* 2007 The Python-based Simulations of Chemistry Framework (PySCF). preprint, available at arXiv, https://arxiv.org/abs/1701.08223v2

[55] Li X and Paldus J 2008 Full Potential Energy Curve for N_2 by the Reduced Multireference Coupled-Cluster Method *J. Chem. Phys.* **129** 054104

[56] Roy R J L, Huang Y and Jary C An Accurate Analytic Potential Function for Ground-State N_2 from a Direct-Potential-Fit Analysis of Spectroscopic Data *J. Chem. Phys.* **125** 164310

[57] Bünemann J, Linneweber T and Gebhard F Approximation schemes for the study of multi - band Gutzwiller wave functions *Phys. Stat. Sol. B* **254** 1600166

[58] Schickling T, Bünemann J, Gebhard F and Boei Lilia Quasiparticle bands and structural phase transition of iron from Gutzwiller density-functional theory *Phys. Rev. B* **93** 205151.

[59] Schickling T, Bünemann J, Gebhard F and Weber W Gutzwiller density functional theory: a formal derivation and application to ferromagnetic nickel *New J. Phys.* **16** 093034.

[60] Farooq Z, Chestakov D A, Yan B, Groenenboom G C, Zande W J and Parker D H 2014 Photodissociation of Singlet Oxygen in the UV Region *Phys.Chem.Chem.Phys.* **16** 3305-3316

[61] Motta M *et al.* 2017 Towards the Solution of the Many-Electron Problem in Real Materials: Equation of State of the Hydrogen Chain with State-of-the-Art Many-Body Methods *Phys. Rev. X* **7** 031059

[62] Casula M and Sorella S 2003 Geminal Wave Functions with Jastrow Correlation: A First Application to Atoms *J. Chem. Phys.* **119** 6500-6511

[63] Casula M, Attaccalite C and Sorella S 2004 Correlated Geminal Wave Function for Molecules: An Efficient Resonating Valence Bond Approach *J. Chem. Phys.* **121** 7110-7126

[64] Neuscamman E 2013 The Jastrow Antisymmetric Geminal Power in Hilbert Space: Theory, Benchmarking, and Application to a Novel Transition State *J. Chem. Phys.* **139** 194105